MAXIMUM-EFFICIENCY GENERALIZED CLASSICAL AXIALLY-SYMMETRIC DUAL-REFLECTOR ANTENNAS

Fernando J. S. Moreira
UFMG - Dept. Electronics Engineering
Av. Pres. Antonio Carlos 6627 - C. P. 209
30161-970 Belo Horizonte, MG, BRAZIL

Aluizio Prata, Jr.
University of Southern California
Dept. Electrical Engineering–Electrophysics
Los Angeles, CA 90089-0271, USA

Abstract

Recent studies have dealt with the design of generalized classical axially-symmetric dual-reflector antennas. These classical configurations are capable of reducing the main-reflector radiation towards the subreflector surface, while providing a uniform-phase aperture field. Using Geometrical Optics principles, closed-form design and aperture-field equations have been derived, in a unified way, for the four distinct types of classical antennas. In the present work, a parametric study is conducted in order to determine the classical geometries yielding maximum radiation efficiency. The results are useful to obtain an optimum starting configuration for a diffraction-shaping procedure.

1. Introduction

Classical axially-symmetric Cassegrain and Gregorian reflectors have a wide variety of high-gain antenna applications [1]. The main drawback of these configurations is the subreflector blockage, which causes a number of deleterious effects such as the decrease of the antenna aperture efficiency. However, this problem can be minimized by either shaping both reflectors or using generalized classical configurations [2]–[4], in order to reduce the main-reflector radiation towards the subreflector.

The generalized classical axially-symmetric dual-reflector antennas have their dishes described by generating curves geometrically represented by conic sections (see Figs. 1–4). Excited by a spherical-wave feed source located at the primary focus, the antennas provide a uniform-phase aperture distribution while avoiding the incidence of main-reflector reflected rays upon the subreflector. These configurations are divided into four different groups, namely Axially Displaced Cassegrain (ADC), Gregorian (ADG), Ellipse (ADE), and Hyperbola (ADH). They are illustrated in Figs. 1–4, respectively. The main difference among the geometries resides on the location of the subreflector caustics. One is a ring caustic defined by the rotation of the parabola focus (point P) around the symmetry axis (z-axis). The other is a line caustic corresponding to the portion of the symmetry axis intercepted by rays reflected from the subreflector (points T). Closed-form design and aperture-field equations have been derived for these classical configurations, based on Geometrical Optics (GO) [3],[4]. The formulation is used in the present work to determine the configurations yielding maximum radiation efficiency, which can be used to start a diffraction-shaping procedure of such antennas.

2. GO Aperture Field Distribution

According with the design procedure of Refs. [3] and [4], the geometry of a given generalized classical axially-symmetric dual-reflector antenna is completely determined by the following input parameters (see Figs. 1–4): the main-reflector, subreflector, and blockage diameters D_M, D_S, and D_B, respectively; the subreflector edge angle θ_E; and the constant path length ℓ_o from the primary focus (point O) to the antenna aperture (assumed at the plane $z = 0$). Once the geometry is specified and assuming a circularly-symmetric raised-cosine feed (RCF) model representing the feed illumination [5], the GO aperture field amplitude is then given by [3]

$$|\vec{E}^A(\rho_A)| = \cos^h \theta_F \sqrt{\left| \frac{\tan(\theta_F/2)\,[A_1(\theta_F) - A_2(\theta_F)]^3}{4F(e^2-1)\,[A_3(\theta_F) - A_4(\theta_F)]} \right|}, \tag{1}$$

where

$$A_1(\theta_F) = (1 - e\cos\beta)(1+\cos\theta_F), \quad A_3(\theta_F) = [c(1-e\cos\beta) + eF]\sin\beta\,(1+\cos\theta_F), \\ A_2(\theta_F) = e\sin\beta\sin\theta_F, \quad A_4(\theta_F) = [F(1+e\cos\beta) + ce\sin^2\beta]\sin\theta_F, \tag{2}$$

$\vec{E}^A$ is the GO aperture electric field, ρ_A is the distance from the z-axis to the aperture point, h controls the circularly-symmetric pattern of the RCF model, θ_F defines the feed-ray direction, e and $2c$ are the eccentricity and interfocal distance of the subreflector conic section, respectively, F is the focal length of the

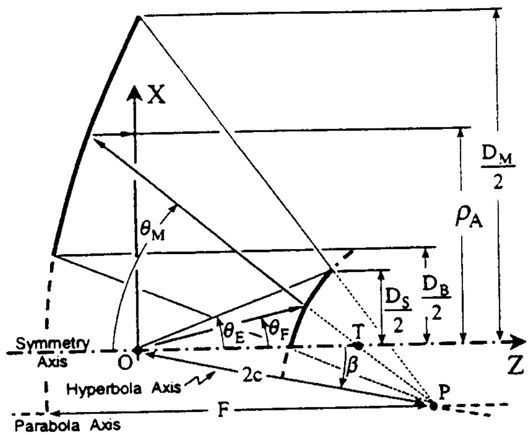

Fig. 1: ADC Configuration.

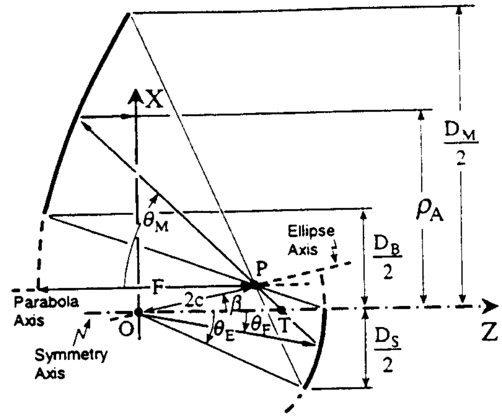

Fig. 2: ADG Configuration.

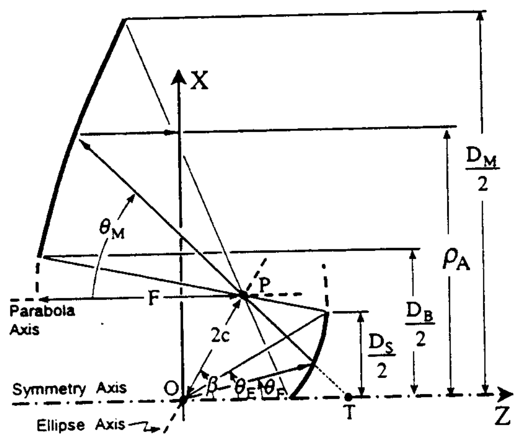

Fig. 3: ADE Configuration.

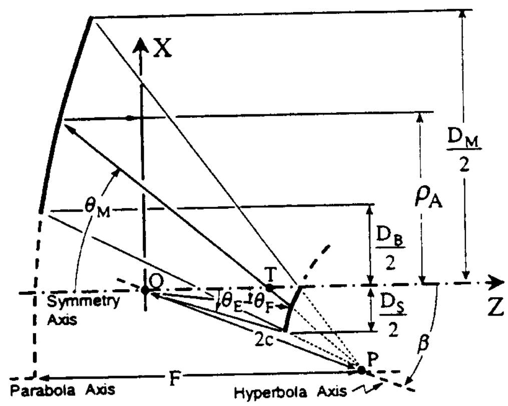

Fig. 4: ADH Configuration.

main-reflector parabola, and β is the tilt angle between the subreflector conic-section axis and the z-axis. The relation between θ_F and ρ_A is given by [3]

$$\tan\left(\frac{\theta_F}{2}\right) = \frac{e\,(\sin\beta + \Delta\,\cos\beta) - \Delta}{e\,(\cos\beta - \Delta\,\sin\beta) + 1}, \qquad \Delta = -\,\tan\left(\frac{\theta_M}{2}\right) = \frac{\rho_A - 2c\,\sin\beta}{2F}. \tag{3}$$

Equations 1–3 are valid for all four classical configurations, as far as one observes that positive (negative) angular values correspond to counterclockwise (clockwise) angles in Figs. 1–4 and that the hyperbolas of the ADC and ADH geometries can be either convex ($e > 1$) or concave ($e < -1$) [3],[4].

3. Maximum-Efficiency Configurations

In this section, a parametric study is conducted in order to determine the geometries providing maximum radiation efficiency. From the previous discussion, the antenna geometry and its associated GO aperture field are completely determined once the parameters D_M, D_S, D_B, θ_E, ℓ_o, and h are specified. Instead of using h to characterize the RCF, it is preferable to define its far-zone amplitude taper F_t towards $\theta_F = \theta_E$, given by $F_t = 20\,h\,\log_{10}(\cos\theta_E)$. The radiation efficiency η is then calculated from the antenna aperture efficiency (with the help of Eq. 1) and from the feed-spillover loss (using the RCF model) [5]. Due to the adopted GO concepts, η is identical for similar antennas when the same feed illumination is applied. An antenna is similar to another if they only differ by a scale factor (in this work, D_M is the scale factor). In order to provide the maximum illuminated aperture area, D_B is always assumed equal to D_S. The parametric study is then carried out by varying the values of D_S/D_M ($0 < D_S/D_M \leq 0.2$), θ_E ($0° < |\theta_E| \leq 60°$), and ℓ_o/D_M ($0.5 \leq \ell_o/D_M \leq 2$). Note that, according with the adopted angular orientation, $\theta_E < 0$ for the ADG and ADH. For each triplet D_S/D_M, θ_E, and ℓ_o/D_M the values of F_t and η (yielding the maximum η) are then

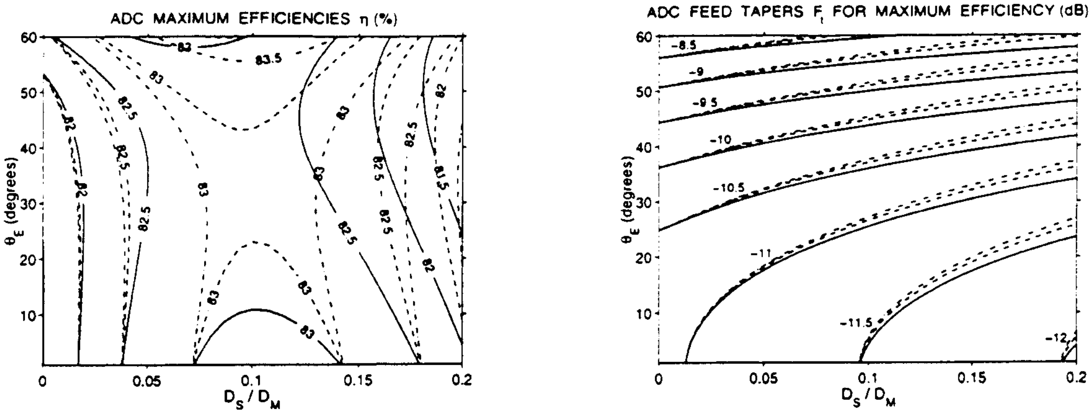

Fig. 5: ADC a) Maximum Efficiencies η and b) Corresponding Feed Tapers F_t: $\ell_o/D_M = 0.5$ (solid lines), 1 (dashed lines), and 2 (dash-dot lines).

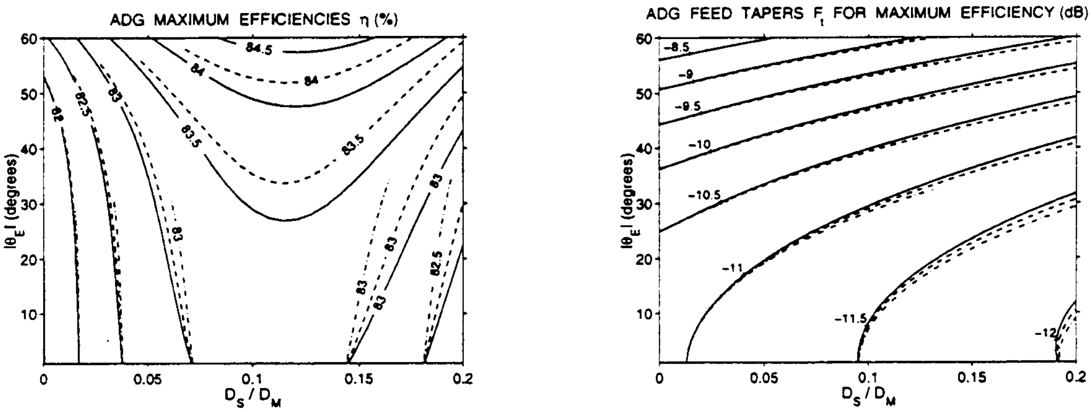

Fig. 6: ADG a) Maximum Efficiencies η and b) Corresponding Feed Tapers F_t: $\ell_o/D_M = 0.7$ (solid lines), 1 (dashed lines), and 2 (dash-dot lines).

obtained. The resulting η values and their associated F_t are shown for the ADC (Fig. 5), ADG (Fig. 6), ADE (Fig. 7), and ADH (Fig. 8) configurations.

The efficiencies of the ADC and ADG approximately have the same behavior (Figs. 5 and 6, respectively). Their maximum values are about 83%, occuring around $D_S/D_M = 0.1$ and with $F_t \approx -11$ dB. These results come with no surprise as, for small D_S/D_M values, the geometries approximate the classical Cassegrain and Gregorian configurations, respectively. Applying the equivalent-paraboloid principle, the maximum $\eta \approx 83\%$ with $F_t \approx -11$ dB is then expected [5]. Feed and self blockages may occur for the ADG. The feed blockage is characterized by the incidence of subreflector reflected rays upon the feed (assumed a point source). The self blockage refers to the intersection of rays reflected by the subreflector lower (upper) half with the subreflector upper- (lower-) half surface. According with the above definitions, these blockages can only occur for the ADG and ADH configurations (see Figs. 1–4). The geometric conditions for the avoidance of these blockage mechanisms are found in Ref. [3]. It was observed for the ADG that, for the adopted range of D_S/D_M and $|\theta_E|$, the feed blockage does not occur when $\ell_o/D_M \geq 0.7$. As the value of ℓ_o/D_M increases, the concern is about the self blockage. When $\ell_o/D_M = 1$, the self blockage appears for small values of D_S/D_M and large $|\theta_E|$ values. For $\ell_o/D_M = 2$, this blockage mechanism occurs whenever $|\theta_E| > 35°$. In Fig. 6 the contour lines are not plotted at regions where the self blockage is at play.

The ADE and ADH provide maximum efficiencies around 91% (see Figs. 7 and 8, respectively), somewhat higher than those obtained by the ADC and ADG. This is due to the converse of the feed energy redistribution in the aperture plane [2]. The results indicate that η increases as $D_S/D_M \to 0$, which permits the use of very small subreflectors without compromising the antenna performance. Furthermore, high efficiencies are obtained in conjunction with large $|F_t|$ values, allowing the achievement of low feed spillovers. However, the self and feed blockages are of great concern for the ADH configuration. The feed blockage stops to occur

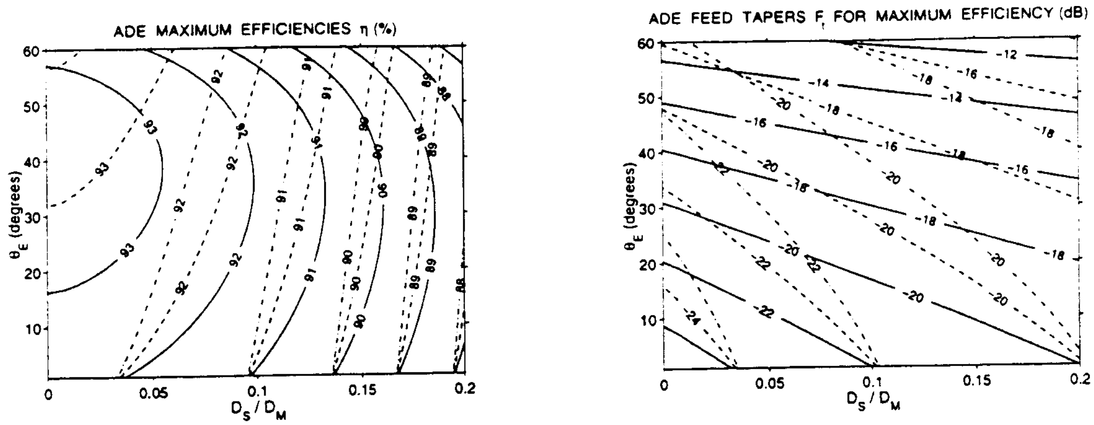

Fig. 7: ADE a) Maximum Efficiencies η and b) Corresponding Feed Tapers F_t: $\ell_o/D_M = 0.5$ (solid lines), 1 (dashed lines), and 2 (dash-dot lines).

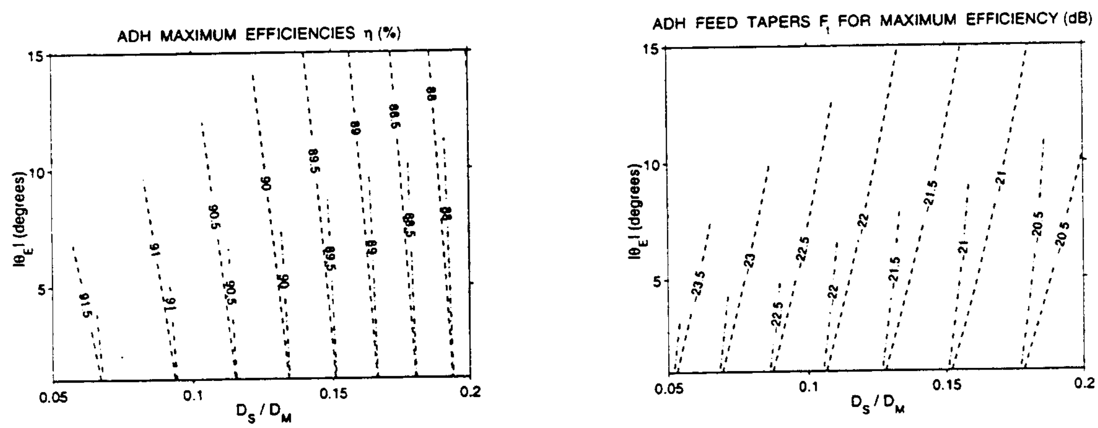

Fig. 8: ADH a) Maximum Efficiencies η and b) Corresponding Feed Tapers F_t: $\ell_o/D_M = 1$ (dashed lines) and 2 (dash-dot lines).

only when $\ell_o/D_M > 0.9$. The self blockage is always present when $|\theta_E| > 20°$. In Fig. 8, the contour lines are interrupted whenever the self blockage is present.

4. Conclusions

This work presented a parametric study to determine the generalized classical axially-symmetric dual-reflector configurations yielding maximum radiation efficiencies. It was observed that, in principle, efficiencies up to 83% can be achieved by the ADC and ADG configurations. They are obtained with about 11 dB feed amplitude taper towards the subreflector edge and for an optimum subreflector diameter approximately ten times smaller than the main-reflector one. The ADE and ADH configurations can achieve efficiencies beyond 90% with smaller subreflector diameters and larger feed tapers (less spillover). However, feed and self blockages are great concerns for the ADG and, specially, for the ADH.

References

[1] W. V. T. Rusch, "The Current State of the Reflector Antenna Art—Entering the 1990's," Proceedings of the IEEE, **80**, No. 1, pp. 113–126, January 1992.

[2] Yu. A. Yerukhimovich, "Analysis of Two-Mirror Antennas of a General Type," Telecommunications and Radio Engineering, Part 2, **27**, No. 11, pp. 97–103, 1972.

[3] F. J. S. Moreira, "Design and Rigorous Analysis of Generalized Axially-Symmetric Dual-Reflector Antennas," Ph.D. Dissertation, Dept. Electrical Engineering, University of Southern California, 1997.

[4] F. J. S. Moreira and A. Prata, Jr., "Generalized Classical Axially-Symmetric Dual-Reflector Antennas," 1997 IEEE AP-S International Symposium Digest, Montreal, Canada, pp. 1402–1405, July 1997.

[5] S. Silver (Ed.), *Microwave Antenna Theory and Design*, Peter Peregrinus, London, 1984.